

Growth and Characterization of Graphene on Polycrystalline SiC Substrate Using Heating by CO₂ Laser Beam

Nierlly Karinni de Almeida Maribondo Galvão^{a*}, Getúlio de Vasconcelos^b,

Marcos Valentim Ribeiro dos Santos^b, Tiago Moreira Bastos Campos^a, Rodrigo Sávio Pessoa^{a,c},

Marciel Guerino^a, Mohamed Abdou Djouadi^d, Homero Santiago Maciel^{b,c}

^a Technological Institute of Aeronautics, Praça Marechal Eduardo Gomes, 50, São José dos Campos, 12228-900, São Paulo, SP, Brazil

^b Institute of Advanced Studies, Photonics Division, Rodovia dos Tamoios, 12.228-001, São Jose dos Campos, SP, Brazil

^c Nanotechnology and Plasma Processes Laboratory, University of Paraíba Valley, 12244-000, São Jose dos Campos, SP, Brazil

^d Institut des Matériaux Jean Rouxel IMN, UMR 6502, Université de Nantes, 1 Quai de Tourville 44035, Nantes Cedex 1, France

Received: April 12, 2016; Revised: July 27, 2016; Accepted: September 04, 2016

The thermal decomposition of silicon carbide (SiC), with the subsequent formation of graphene, can be achieved by heating treatment. Several heating processes have been applied for this purpose by using SiC, either in form of powder particles or monocrystalline substrate. In this work, instead of using an expensive commercially available SiC wafer, a polycrystalline SiC substrate was obtained, based on powder metallurgy process, in order to explore the synthesis of graphene layers on its surface by using a CO₂ laser beam as heating source. Different levels of energy density (fluence) were applied and Raman spectroscopy analyses demonstrated that graphene layers were formed on the polycrystalline SiC surface. The ratio of the integrated intensity of the D and G bands, and the crystallite size were calculated. The FWHM of the 2D band peaks are in excellent agreement with the range of values found in the literature. The samples irradiated with energy density of 138.4 J/cm² presented lower concentration of defects and higher crystallite size, while the lowest FWHM was obtained for energy density of 188 J/cm². The process occurred at room conditions and no gas flow was used. The results reveal a simple and cost-effective alternative for synthesis of graphene-based structures on SiC.

Keywords: Polycrystalline SiC; Graphene; CO₂ laser heating; SiC thermal decomposition; Raman spectroscopy

1. Introduction

An allotropic form of the carbon, graphene is basically constituted by a monolayer of sp² carbon atoms arranged in a two-dimensional hexagonal lattice¹⁻³. Graphene is a zero-band gap semiconductor and exhibits exceptional physical properties due to its extremely high carrier mobility²⁻⁶. As a result of its remarkable properties, the graphene has been widely studied in last years. Several techniques have been used to synthesize the graphene, such as mechanical exfoliation^{1,7}, chemical exfoliation^{8,9}, chemical vapor deposition (CVD)^{10,11}, chemical reduction of graphite oxide¹², growth on transition metals^{13,14}, and thermal decomposition of SiC, that allows to synthesize an epitaxial graphene¹⁵⁻²².

Several papers report the growth of epitaxial graphene on SiC by thermal decomposition in induction furnaces operating at vacuum or at atmospheric pressure with an inert gas flow. In such methods, the sample should achieve

temperatures sufficiently high to break the Si-C bands at the upper crystalline layers of SiC. Therefore, Si atoms will be sublimated and the graphitization will be able to occur, where the C atoms on the top of surface are rearranged to synthesize the epitaxial graphene^{4,16-19}. In order to create alternative processes, some studies have shown that the addition of a layer of “catalyst material” (such as Ni or Co) promotes the reduction of the temperature required for SiC decomposition²³⁻²⁶. Nevertheless, despite SiC dissociation is promoted in this case, the Si sublimation does not occur; rather a chemical reaction to form a silicide phase between the catalyst material and Si happens.

Recently, some works reported the use of lasers as heating sources to obtain the epitaxial graphene on SiC. Lee S. et al.²⁷ reported the growth of epitaxial graphene on SiC wafer through the use of a pulsed UV-laser in a vacuum chamber at approximately 10⁻⁶Torr. Yannopoulos et al.²⁸ reported the use of a CO₂ laser with Ar gas flow, with fast heating, followed by a high cooling rate. In their process, the C-face of SiC wafer was

* e-mail: nierlly@gmail.com

irradiated, but the graphene grew epitaxially at the opposite face (Si-face). It is worth noting that such process did not require either vacuum or pre-treatment. These authors suggested that graphene did not grow on the C-face (face directly exposed to the CO₂ laser beam) because the partial pressure of oxygen was significantly higher on this face in comparison with Si-face²⁸. The process of the graphene growth with CO₂ laser in atmospheric pressure was also performed by Antonelou et al.²⁹, aiming to obtain 3D graphene froths from SiC particles. These studies show that the use of laser as a heating source for the SiC thermal decomposition to produce graphene is viable and promising. It is important to highlight that an advantage of this technique is the possibility to create tracks or more complex shapes of graphene on SiC surface without need of a prior lithography. Nevertheless, the investigations of this process are in the early stages, thus more studies are desirable concerning, for example, the effect of laser energy density and morphology of the substrate surface on the formation of graphene by thermal decomposition of the SiC.

In this context, this work presents studies about the growth and characterization of graphene layers on sintered polycrystalline SiC substrate by using heating by CO₂ laser beam. Such investigation is even more interesting since it can bring useful information to achieve our further goal, i.e. to induce, by using laser heating, the synthesis of graphene on thin films of polycrystalline SiC grown by plasma sputtering technique. Besides, it allows to check the applicability of this technique to grow graphene on polycrystalline SiC, rather than on expensive crystalline SiC wafer. Here, the main process parameter was the energy density applied for heating the substrate and sublimation of the Si with consequent formation of graphene layers. The produced graphene was characterized by Raman spectroscopy and field emission scanning electron microscopy (FESEM). The whole process was performed under a stagnant atmospheric environment and heating and cooling occurred at standard conditions.

2. Experimental

2.1. SiC samples preparation

SiC substrates were produced by powder metallurgy technique. β -SiC powder GRADE BF-12 type from C. Hermann Starck (HCST) was used. For liquid phase sintering, different additives were added to the powder mixture: YAG (Yttrium Aluminium Garnet) - 7.6% by mass, the PVA binder (polyvinyl alcohol), manufactured by VETEC Química Fina do Brasil, and Bio de flocculant Denvercil 300 produced by DENVER Resinas. For compression, an uniaxial pressing at a load of 40 MPa and an isostatic pressing at a load of 300 MPa were applied. The SiC samples were sintered at 1900°C in argon atmosphere, as described in the literature³⁰.

2.2. Si sublimation by CO₂ laser heating

The heating of the samples was performed through the use of CO₂ laser beam (*Synrad Evolution - 125*) with 125 W and beam diameter of 200 μ m, which emits infrared laser radiation in the 10.6 μ m wavelength band. The samples were positioned at the focal region of the laser, as illustrated in Figure 1. For all samples, 100% of the laser power and a beam overlap of 50% were used. Nevertheless, in order to change the energy density applied to the samples, different scanning velocities of the laser beam were used. Table 1 shows each scanning velocity used and the correspondent energy density.

2.3. Material characterization

Raman spectroscopy measurements were performed using a Renishaw system model 2000 equipped with an Ar ion laser (514.5 nm). Raman spectra were obtained at room temperature in the range of 450 to 2800 cm⁻¹ for analyses of the SiC substrate and 1200 to 1700 cm⁻¹ and 2400 to 2900 cm⁻¹ for the graphene. For more accurate results, the baseline of each spectrum was subtracted to highlight the areas and intensities of the peaks.

Many authors have shown that it is possible to obtain from Raman analysis the inherent features of the graphene, including structural quality and the number of layers^{23,31-33}. Raman spectra obtained by laser excitation at 2.41 eV have shown that the G and 2D bands, which appear at approximately 1582 cm⁻¹ and 2700 cm⁻¹, respectively, are the main features of a monolayer graphene³¹. The G band is associated with the E_{2g} phonon mode at the Brillouin zone center, and this band originated from the first order Raman Scattering. The 2D band is originated from second-order, which involves the two Brillouin zone boundaries^{23,31}. In some cases, the D band at ~1350 cm⁻¹ and the less intensive peaks of the D' band at ~1620 cm⁻¹ also appear. This D and D'-bands comes from double-resonant processes and they are related to the presence of defects and structural disorder in graphene^{31,32}. Therefore, the relative integrated intensity (area) ratio of the D and G bands, A(D)/A(G), in some works presented as I_D/I_G, is used to evaluate the defect concentration of the graphene films²⁵. From the A(D)/A(G) ratio, it is possible to determine the crystallite size, L_a, by using Eq. 1,

$$L_a \text{ (nm)} = \frac{560}{E_1^4} \left(\frac{A(D)}{A(G)} \right)^{-1} \quad (1)$$

where E₁ is the excitation laser energy of Raman, in eV³³.

The surface morphology of the SiC substrate, as well as of its surface coated with the produced graphene, was examined by using Field Emission Scanning Electron Microscopy -FESEM (Mira 3 from Tescan).

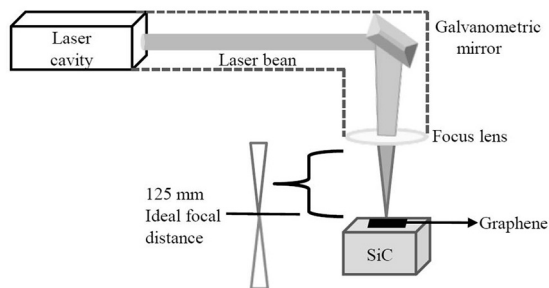


Figure 1: Schematic diagram of the laser irradiation process. During the process, the samples were positioned at the focal distance of 125 mm.

3. Results

Figure 2 shows the X-Ray Diffraction (XRD) and Raman spectra of the sintered polycrystalline SiC. The XRD spectra, Figure 2(a), showed a characteristic spectrum of SiC with major peaks at (111), (220), (311) and (200) respectively. For the Raman spectra, Figure 2(b), peaks referent to the Si-C band appear at ~ 796 and 970 cm^{-1} . The peaks overlapping the C-C band (G and D) and the second order Raman spectra of the SiC also appear at regions ~ 1315 - 1362 cm^{-1} and 1524 - 1574 cm^{-1} . However, the peaks referent to the C band are broad and not well defined. Peaks related to 2D band (2700 cm^{-1}) were not observed.

Figure 3 presents the Raman spectra of graphene synthesized on the polycrystalline SiC for different values of energy density. The peaks of the fundamental vibration modes of graphene, D and G bands, and 2D band appear at ~ 1355 , 1581 - 1607 , and $\sim 2709\text{ cm}^{-1}$, respectively. Unlike reported in some studies where SiC (0001) was used as a substrate, the Raman spectra obtained in the present work did not show any interference signals from SiC. Possibly this is related to the polycrystalline SiC used. Figure 3 clearly shows that there is no overlapping of the peaks of SiC and C bands in any of the results. The D and G band peaks are well defined, showing that, although the process has been done at room conditions, the graphene oxide is absent. By considering the vapor-emitting surface effect described by Schiller et al.³⁴, it is possible to conclude that, in the present process, it is unlikely that the graphene suffers oxidation. When Si is removed from the system, the Si vapor stream drags out the present gas (atmospheric air) surrounding the material surface, what prevents the contact of the oxygen with the carbon atoms of the SiC surface. Also, for oxidation process to occur, it requires the effective collision between the sublimed Si and oxygen in the air. Therefore, due to the drag and the fact that the process happens in a short period of time, the resulting C in surface comes back to

room temperature and there is not enough energy for the carbon oxidation reaction to occur. Also in Figure 3, the D band, which is representative of disorder and/or defects, was systematically observed. Unlike the graphene obtained by micromechanical cleavage from Highly Ordered Pyrolytic Graphite (HOPG), the graphene grown from crystalline SiC usually has defects (D-band)^{22,23,35,36}. Because polycrystalline SiC was used in the present work for graphene growth, the presence of defects was expected. The defect concentration, $A(D)/A(G)$, and the crystallite sizes, L_a , are presented in Figure 4. Eckmann et al.³⁷ investigated different types of graphene defects by mean of Raman spectroscopy. A relation between the ratio of the peaks intensity (peaks height) D and D', $I(D)/I(D')$, and the type of defects in graphene was proposed: $I(D)/I(D')$ is maximum (~ 13) for sp³-defects, (~ 7) for vacancy-like defects and, (~ 3.5) for boundaries defects. In our samples we obtained $I(D)/I(D')$ ratios of ~ 1.7 and ~ 3.61 , for samples irradiated with energy density of 200 J/cm^2 and 138.4 J/cm^2 , respectively, indicating a high concentrations of boundaries defects. Also, as pointed out in Eckmann et al.³⁷, when a graphene sample has high concentration of defects, the D' peak is somehow merged with the G peak, which is observed in our samples. Therefore, to obtain the correct height of both peaks a Lorentzian double peaks function was applied to the data.

As shown in Figure 4, only a slight increase in defect concentration could be seen when the polycrystalline SiC was irradiated from 138.4 J/cm^2 to 188.0 J/cm^2 . Accordingly, calculated L_a decreases from $61,48\text{ nm}$ to $41,5\text{ nm}$ when the polycrystalline SiC was irradiated from 138.4 J/cm^2 to 188.0 J/cm^2 . As previously commented, L_a represents the crystallite size of the graphene regions, which depends on the defect concentration. However, for L_a analysis, it is also important to consider the influence of the morphology of the SiC substrate surface. The graphene produced appears as small "islands" and not as a continuous large layer, as shown in the FESEM images, Figure 4. Probably due to the non-uniform structure of the uppermost layer of the polycrystalline SiC and to the presence of pores, as illustrated in Figure 4(a), the extension of the formed graphene layers is limited, producing a non-continuous coating over the substrate surface.

It is worth mentioning that the heat transfer along and across the heterogeneous surface, as in the present case, may cause non-uniformity of temperature distribution on the surface, which is another factor that may influence the thermal dissociation of SiC, so affecting locally the graphene formation. Furthermore, the terminations of the SiC grains may be another source of defect concentration for the graphene islands, influencing the L_a values. Therefore, the laser fluence may not be the only factor responsible for the

Table 1: Scanning velocities and energy applied at the samples.

Scanning velocities (mm/s)	800	850	900	950	1000	1150	1200
Energy density(J/cm^2)	200.0	188.0	177.6	168.0	160.0	138.4	132.8

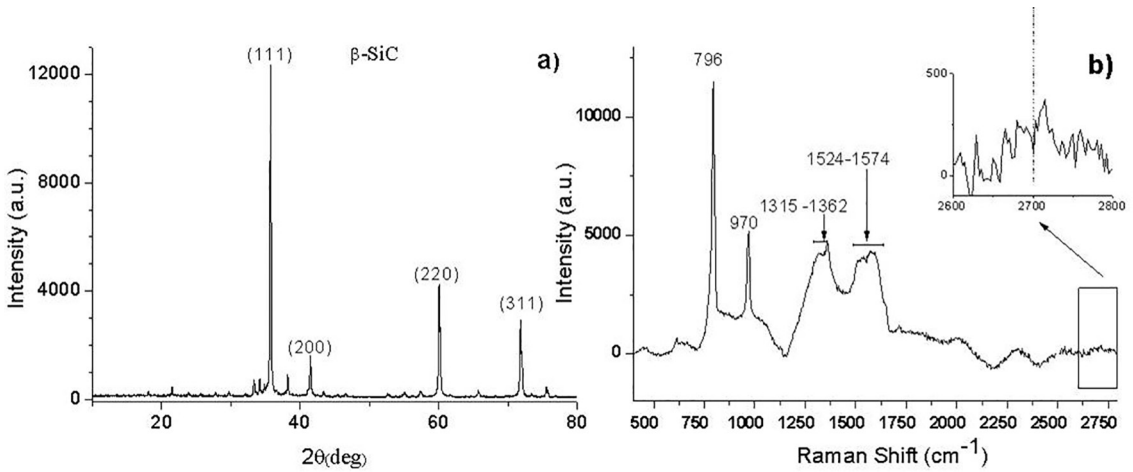


Figure 2: (a) X-ray diffraction spectra of SiC sintered; (b) Raman spectra of the polycrystalline SiC substrate.

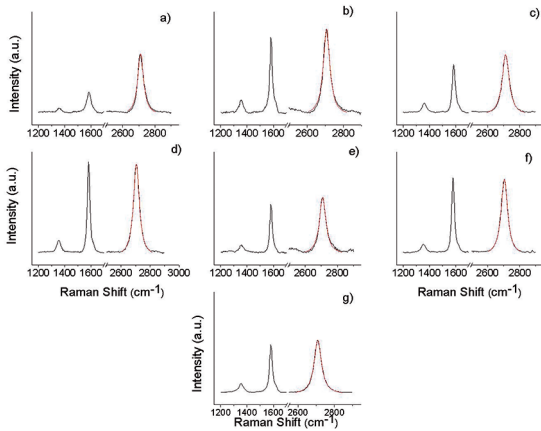


Figure 3: (color online) Raman spectra of graphene grown on SiC for different condition of energy density applied at the samples during laser irradiation. a) 200.0 J/cm², b) 188.0 J/cm², c) 177.6 J/cm², d) 168.0 J/cm², e) 160.0 J/cm², f) 138.4 J/cm², and g) 132.8 J/cm². The black line represents the experimental results and the red line the 2D band peak fitted by Lorentz function.

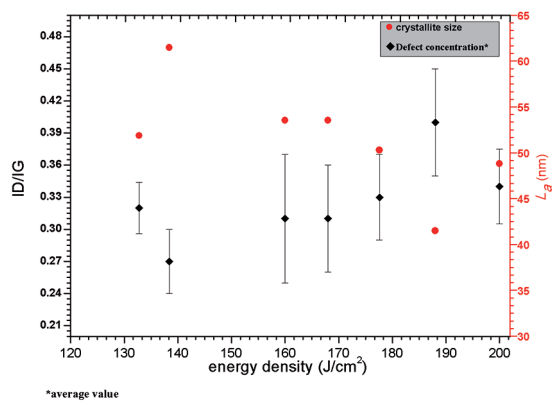


Figure 4: Relation between defect concentration, $A(D)/A(G)$, and the crystallite sizes, L_a , with the laser energy density applied for synthesis of the graphene.

discrepancy between the conditions with lowest and highest concentration of defects, i.e., the polycrystalline structure also affects the defect concentration of formed graphene and, therefore, the L_a value.

Figure 5(a) shows the surface of the untreated polycrystalline SiC substrate. In Figure 5(b), small graphene islands on SiC grains can also be seen. When the FESEM resolution was increased, it was possible to see more precisely the graphene shape, as shown in Figure 5(c). These FESEM images were obtained for the sample that presented the highest L_a (irradiated with energy density of 138.4 J/cm²). It is possible to see in Figure 5 (c) that the size of the grains is comparable with the L_a calculated, including errors bars.

FWHM was obtained from the Lorentz fitting of the 2D band peak, from which the number of graphene layers can be inferred. As reported in literature, for a monolayer graphene, obtained by mechanical exfoliation, the FWHM was lower than 30 cm^{-1} ^{31,38}. Using a Raman laser of 488 nm, Lee D.S et al.³⁸ reported that due to the intrinsic disorder of the monolayer epitaxial graphene (grown on a Si terminated face of SiC), the FWHM was found at approximately 46 cm^{-1} , which is higher than that for exfoliated graphene. Lee D.S. et al.³⁸ also reported results for the bi- and tri-layer graphene that exhibit a FWHM at approximately 64 cm^{-1} and 74 cm^{-1} , respectively. The FWHM of the graphene obtained in our process was found in the range between 43.5 cm^{-1} and 49.5 cm^{-1} . Although the results are close to those found for the monolayer epitaxial graphene, it is not possible to conclude that there is only one monolayer, since the FWHM depends on several factors such as strain, doping, point defects, heterogeneities, grain size, and stacking order^{39,40,41}.

4. Conclusion

Polycrystalline SiC substrate was used for the first time to synthesize graphene by means of thermal decomposition

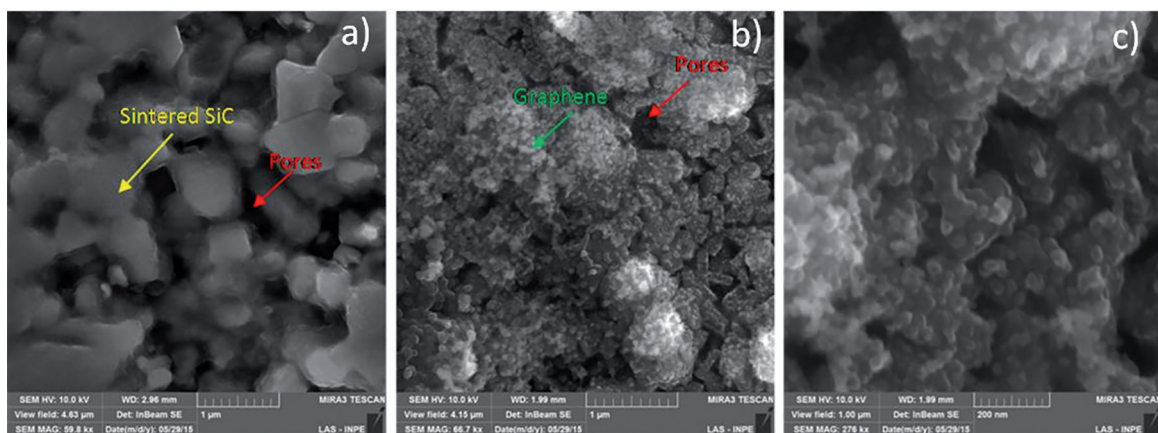


Figure 5: (color online) FESEM images: a) polycrystalline SiC substrate; b), and c) graphene synthesized with energy dose of 138.4 J/cm².

process using CO₂ laser beam as heating source. Raman spectroscopy proved that graphene was formed on the surface of the porous and non-oriented SiC substrate. FESEM images confirm these results and show that graphene layers appear as small “islands” on top of SiC grains, spread all over the substrate surface, and not as a continuous layer as usually happens in the case of monocrystalline SiC. Graphene, free of oxidation, was synthesized for all tested conditions of laser energy density with no significant difference in the obtained material features. Such results demonstrate that the CO₂ laser heating treatment, of low cost sintered SiC, is a handy and cost-effective alternative process for coating polycrystalline SiC with graphene based nanostructures, which could be interesting for applications in different areas as, for example, solid lubricants in the field of nanotribology.

5. Acknowledgements

This work was supported by the Brazilian funding agency CAPES, grants No. 23038.005802/2014-98 and No. 88881.064970/2014-01, CNPq, grants No 473043-2012, and São Paulo Research Foundation (FAPESP), grant No. 2011/07468-2 and (FAPESP/CNPq/PRONEX) No. 2011/50773-0. We also would like to thanks to the Prof. Dr. Stanislav Moshkalev for the assistance, LAS-IMPE for RAMAN measurements, and Maria Lucia Brison - LAS-IMPE, for the FESEM images.

6. References

- Novoselov KS. Nobel Lecture: Graphene: Materials in the flatland. *Reviews of Modern Physics*. 2011;83(3):837-849.
- Novoselov KS, Geim AK, Morozoy SV, Jiang D, Zhang Y, Dubonos SV, et al. Electric field effect in atomically thin carbon films. *Science*. 2004;306(5696):666-669.
- Geim AK, Novoselov KS. The rise of graphene. *Nature Materials*. 2007;6:183-191.
- Avouris P, Dimitrakopoulos C. Graphene: synthesis and application. *Materials Today*. 2012;15(3):86-97.
- Yechika Y. Application of graphene to high-speed transistors: expectations and challenges. *Science & Technology Trends*. 2010;37:76-92.
- Huang X, Yin Z, Wu S, Qi X, He Q, Zhang Q, et al. Graphene-based materials: synthesis, characterization, properties, and applications. *Small*. 2011;7(14):1876-1902.
- Tang Q, Zhou Z. Graphene-analogous low-dimensional materials. *Progress in Materials Science*. 2013;58(8):1244-1315.
- Lotya M, Hernandez Y, King PJ, Smith RJ, Nicolosi V, Karlsson LS, et al. Liquid phase production of graphene by exfoliation of graphite in surfactant/water solutions. *Journal of the American Chemical Society*. 2009;131(10):3611-3620.
- Khan U, O'Neill A, Lotya M, De S, Coleman JN. High-concentration solvent exfoliation of graphene. *Small*. 2010;6(7):864-871.
- Qi JL, Zheng WT, Zheng XH, Wang X, Tian HW. Relatively low temperature synthesis of graphene by radio frequency plasma enhanced chemical vapor deposition. *Applied Surface Science*. 2011;257(15):6531-6534.
- Choi T, Jung H, Lee CW, Mun KY, Kim SH, Park J, et al. Growth characteristics of graphene synthesized via chemical vapor deposition using carbon tetrabromide precursor. *Applied Surface Science*. 2015;343:128-132.
- Dao TD, Jeong HM. Graphene prepared by thermal reduction-exfoliation of graphite oxide: Effect of raw graphite particle size on the properties of graphite oxide and graphene. *Materials Research Bulletin*. 2015;70:651-657.
- Batzill M. The surface science of graphene: Metal interfaces, CVD synthesis, nanoribbons, chemical modifications, and defects. *Surface Science Reports*. 2012;67(3-4):83-115.
- Grandthyll S, Gsell S, Weinl M, Schreck M, Hüfner S, Müller F. Epitaxial growth of graphene on transition metal surfaces: chemical vapor deposition versus liquid phase deposition. *Journal of Physics: Condensed Matter*. 2012;24(31):314204.
- Trabelsi ABG, Ouerghi A, Kusmartseva OE, Kusmartsev FV, Oueslati M. Raman spectroscopy of four epitaxial graphene layers: Macro-island grown on 4H-SiC₍₀₀₀₁₎ substrate and an associated strain distribution. *Thin Solid Films*. 2013;539:377-383.

16. Gupta B, Notarianni M, Mishra N, Shafiei M, Iacopi F, Motta N. Evolution of epitaxial graphene layers on 3C SiC/Si (111) as a function of annealing temperature in UHV. *Carbon*. 2014;68:563-572.
17. Tang J, Kang CY, Li LM, Pan HB, Yan WS, Wei SQ, et al. Graphene grown on sapphire surface by using SiC buffer layer with SSMBE. *Physics Procedia*. 2012;32:880-884.
18. Heer WA, Berger C, Wu X, First PN, Conrad EH, Li X, et al. Epitaxial graphene. *Solid State Communications*. 2007;143(1-2):92-100.
19. Röhrh H, Hundhausen M, Emtsev KV, Seyller Th, Graupner R, Ley L. Raman spectra of epitaxial graphene on SiC(0001). *Applied Physics Letters*. 2008;92:201918.
20. Seyller T. Epitaxial Graphene on SiC(0001). In: Raza H, ed. *Graphene Nanoelectronics: Metrology, Synthesis, Properties and Applications*. Berlin: Springer-Verlag; 2012. p. 135-145.
21. Yakimova R, Iakimov T, Yazdi GR, Bouhafis C, Eriksson J, Zakharov A, et al. Morphological and electronic properties of epitaxial graphene on SiC. *Physica B: Condensed Matter*. 2014;439:54-59.
22. Zhang R, Li H, Zhang ZD, Wang ZS, Zhou SY, Wang Z, et al. Graphene synthesis on SiC: Reduced graphitization temperature by C-cluster and Ar-ion implantation. *Nuclear Instruments and Methods in Physics Research Section B: Beam Interactions with Materials and Atoms*. 2015;356-357:99-102.
23. Macháč P, Fidler T, Cichoň S, Mišková L. Synthesis of graphene on SiC substrate via Ni-silicidation reactions. *Thin Solid Films*. 2012;520(16):5215-5218.
24. Macháč P, Cichoň S, Mišková L, Vondráček M. Graphene preparation by annealing of Co/SiC structure. *Applied Surface Science*. 2014;320:544-551.
25. Escobedo-Cousin E, Vassilevski K, Hopf T, Wright N, O'Neill A, Horsfall A, et al. Local solid phase growth of few-layer graphene on silicon carbide from nickel silicide supersaturated with carbon. *Journal of Applied Physics*. 2013;113(11):114309.
26. Li C, Li D, Yang J, Zeng X, Yuan W. Preparation of Single- and Few-Layer Graphene Sheets Using Co Deposition on SiC Substrate. *Journal of Nanomaterials*. 2011;2011:319624.
27. Lee S, Toney MF, Ko W, Randel JC, Jung HJ, Munakata K, et al. Laser-Synthesized Epitaxial Graphene. *ACS Nano*. 2010;4(12):7524-7530.
28. Yannopoulos SN, Siokou A, Nasikas NK, Dracopoulos V, Ravani F, Papatheodorou GN. CO₂-Laser-Induced Growth of Epitaxial Graphene on 6H-SiC(0001). *Advanced Functional Materials*. 2012;22(1):113-120.
29. Antonelou A, Dracopoulos V, Yannopoulos SN. Laser processing of SiC: From graphene-coated SiC particles to 3D graphene froths. *Carbon*. 2015;85:176-184.
30. Abdalla AJ, Damião AJ, Campos E, Santana JGA, Vicentini MC, Trevisan TA, et al. Development of Silicon Carbide Substrates for Aerospace Applications. *MRS Proceedings*. 2012;1373:31-36.
31. Malard LM, Pimenta MA, Dresselhaus G, Dresselhaus MS. Raman spectroscopy in graphene. *Physics Reports*. 2009;473(5-6):51-87.
32. Pimenta MA, Dresselhaus G, Dresselhaus MS, Caňado LG, Jorio A, Saito R. Studying disorder in graphite-based systems by Raman spectroscopy. *Physical Chemistry Chemical Physics*. 2007;9(11):1276-1291.
33. Caňado LG, Takai K, Enoki T, Endo M, Kim YA, Mizusaki H, et al. General equation for the determination of the crystallite size L_c of nanographite by Raman spectroscopy. *Applied Physics Letters*. 2006;88(16):163106.
34. Schiller S, Heisig U, Panzer S. *Electron Beam Technology*. New York: John Wiley & Sons; 1982.
35. Ni ZH, Chen W, Fan XF, Kuo JL, Yu T, Wee ATS, et al. Raman spectroscopy of epitaxial graphene on a SiC substrate. *Physical Review B*. 2008;77(11):115416.
36. Hao Y, Wang Y, Wang L, Ni Z, Wang Z, Wang R, et al. Probing layer number and stacking order of few-layer graphene by Raman spectroscopy. *Small*. 2010;6(2):195-200.
37. Eckmann A, Felten A, Mishchenko A, Britnell L, Krupke R, Novoselov KS, et al. Probing the Nature of Defects in Graphene by Raman Spectroscopy. *Nano Letters*. 2012;12(8):3925-3930.
38. Lee DS, Riedl C, Krauss B, von Klitzing K, Starke U, Smet JH. Raman Spectra of Epitaxial Graphene on SiC and of Epitaxial Graphene Transferred to SiO₂. *Nano Letters*. 2008;8(12):4320-4325.
39. Tiberj A, Camara N, Godignon P, Camassel J. Micro-Raman and micro-transmission imaging of epitaxial graphene grown on the Si and C faces of 6H-SiC. *Nanoscale Research Letters*. 2011;6:478.
40. Kumar B, Baraket M, Paillet M, Huntzinger JR, Tiberj A, Jansen AGM, et al. Growth protocols and characterization of epitaxial graphene on SiC elaborated in a graphite enclosure. *Physica E: Low-dimensional Systems and Nanostructures*. 2016;75:7-14.
41. Caňado LG, Jorio A, Pimenta MA. Measuring the absolute Raman cross section of nanographites as a function of laser energy and crystallite size. *Physical Review B*. 2007;76(6):064304.